Hindawi Publishing Corporation
Advances in Meteorology
Volume 2015, Article ID 318608, 9 pages
http://dx.doi.org/10.1155/2015/318608

Research Article

Operational Monitoring of Trace Gases over the Mediterranean Sea

Giuseppe Grieco,[1] Guido Masiello,[2] and Carmine Serio[2]

[1]*Agenzia Spaziale Italiana, Contrada Terlecchia, 75100 Matera, Italy*
[2]*Scuola di Ingegneria, Università degli Studi della Basilicata, Via dell'Ateneo Lucano, 85100 Potenza, Italy*

Correspondence should be addressed to Giuseppe Grieco; giuseppe.grieco@est.asi.it

Received 18 February 2015; Revised 24 April 2015; Accepted 27 April 2015

Academic Editor: Liangfu Chen

This paper describes the operational implementation of the processor φ-IASI over the Mediterranean sea. The φ-IASI model implements two physically based inversion algorithms for the sequential retrieval of (a) the thermodynamic state of the atmosphere and (b) the tropospheric content of CO, CO_2, CH_4, and N_2O from hyperspectral radiance observations of the Infrared Atmospheric Sounding Interferometer (IASI). The retrieval algorithm for trace gases exploits the concept of *partially scanned interferogram* technique, which is a tool mostly suited for Fourier transform spectrometers in the infrared. Minor and trace gases retrievals for July 2010 are presented and compared to in situ observations from five Mediterranean, permanent, stations of the Global Atmospheric Watch (GAW) network. The comparison evidences a good general consistency between satellite and in situ observations. IASI retrievals show a marked southeastern gradient, which is shown to be consistent with the general tropospheric circulation over the Mediterranean basin. These patterns are barely seen from in situ observations, a fact which stresses the importance of satellite (trace gases) data assimilation to improve the performance and quality of trace gases transport models.

1. Introduction

The Infrared Atmospheric Sounding Interferometer (IASI) is a Michelson interferometer developed by the European Agency for the Exploitation of Meteorological Satellites (EUMETSAT). It has been flying onboard the polar Metop A/B orbiting platforms since October 2006 [1]. IASI sounds the atmosphere in the infrared spectral band between 645 cm^{-1} (15.5 μm) and 2760 cm^{-1} (3.6 μm) with a spectral sampling of 0.25 cm^{-1} with the aim of retrieving the thermodynamic state of the atmosphere and its chemical composition for both weather and climate applications. The high quality hyperspectral radiances acquired by IASI [1] allows us to retrieve the thermodynamic structure of the atmosphere with a vertical resolution of 1-2 Km and an accuracy of 1 K for the atmospheric temperature, an accuracy of 0.5 K for the skin temperature, and an accuracy of 10–20% for what concerns the vertical structure of water vapor. These retrieval accuracies meet the World Meteorological Organization (WMO) requirements and, generally, they can be achieved by applying physically based retrieval algorithms [2].

In this paper, we present an operational implementation of the physically based forward/inverse model, called φ-IASI [3, 4], for the Mediterranean Sea. The φ-IASI model is a physically based retrieval package for the estimation of the thermodynamic structure of the atmosphere (surface temperature (T_s), temperature (T), water vapour mixing ratio (H_2O), and ozone mixing ratio (O_3) profiles) and the tropospheric columnar content of minor and trace gases, namely, CO, CO_2, CH_4, and N_2O, from clear sky radiance measurements acquired by IASI.

The limb-sounding of upper and lower stratosphere trace species is amongst the main goals of many satellite missions, for example, Atmospheric Chemistry Experiment (see, e.g., http://www.ace.uwaterloo.ca/) and MIPAS (Michelson Interferometer for Passive Atmospheric Sounding) of the

European Space Agency (see, e.g., https://earth.esa.int/web/guest/missions/esa-operational-eo-missions/envisat/instruments/mipas). However, our study focuses on the retrieval of trace gases from IASI, which is a nadir-looking instrument.

The subject of remote sensing of atmospheric minor and trace gases from nadir-looking instruments on board polar satellites is not a new subject. Instruments used for this objective include the Japanese IMG (Interferometric Monitor for Greenhouse Gases) [5], the American AIRS (Atmospheric Infrared Radiometer Sounder) [6–8], the European IASI [9–17], and the Japanese GOSAT (Greenhouse Gases Observing Satellite) [18].

In this study we offer a different perspective focusing on the use of the partially scanned interferogram (PSI) methodology, first introduced by [19], and demonstrating its capability of achieving columnar contents of trace gases with an unprecedented precision [20]. IASI retrievals for July 2010 over the Mediterranean basin will be compared with in situ observations of the GAW (Global Atmospheric Watch) network. The retrieval exercise will also deserve to get better insight into understanding whether satellite observations of heavy molecules, such as CO_2 and N_2O, can track synoptic-scale weather patterns as claimed by Chahine et al. [7].

The paper is organized as follows. Section 2 gives a description of the modules of the φ-IASI package. Section 3 describes and discusses the results of a retrieval exercise for July 2010; the same section also deals with an analysis of the computing performance of the code. Conclusions are drawn in Section 4.

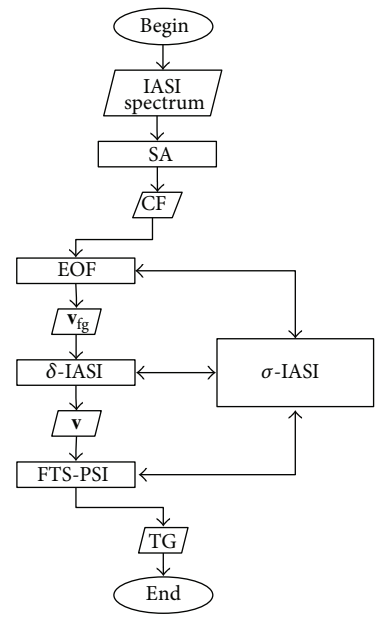

Figure 1: Flow chart of φ-IASI. The acronym SA stands for scene analysis and its output CF stands for cloud flag. $\mathbf{v}$ stands for the thermodynamic state of the atmosphere (T_s, T, H_2O, O_3) while the subscript fg is the acronym for first guess. FTS-PSI stands for Fourier transform spectroscopy with partially scanned interferogram. Finally the acronym TG stands for trace gases. The double-way arrows connecting the modules EOF, δ-IASI, and FTS-PSI with σ-IASI mean that all these modules use the σ-IASI code as a subroutine.

2. The φ-IASI Forward/Inverse Software Package

In this section we summarize the main methodological aspects regarding the algorithms implemented in φ-IASI. An in-depth description of φ-IASI and its accuracy and validation has been presented in many papers [2–4, 21], which the interested reader is referred to for further details.

The model φ-IASI is a MATLAB written software package which consists of seven modules which sequentially process the clear sky spectral radiance observations acquired by IASI. These include a scene analysis module to select only clear sky measurements; an Empirical Orthogonal Functions (EOF) statistical regression scheme to provide the first guess for the next module, which implements an iterative optimal estimation algorithm that we call δ-IASI [4]. The inverse module δ-IASI uses a physical radiative transfer model, which is provided by the module σ-IASI [3]. The two modules δ-IASI and σ-IASI are the core of the φ-IASI model. Once δ-IASI has provided the thermodynamic state of the atmosphere (T_s, T, H_2O, O_3); this state forms the input for each of the modules dedicated to the computation of the total columnar content of minor and trace gases, that is, CO, CO_2, CH_4, and N_2O. The flow chart of φ-IASI is shown in Figure 1. Further details about the individual modules are given below.

2.1. The Scene Analysis Module. The high spectral resolution of new advanced infrared sensors has resulted in better coverage and significantly improved temperature and moisture soundings capabilities compared with the current situation. Infrared data from nadir-looking instruments, however, are frequently affected by clouds. Thus, observations must be processed for operational data assimilation and inversion for geophysical parameters by screening to remove cloud-contaminated soundings. This operation is performed with a *Scene Analysis* module, which is normally based on thresholding of a suitable radiance channels. The scene analysis module embedded in φ-IASI has been variously described in many papers. The most up-to-date version of the module can be found in [22].

2.2. The σ-IASI Code. The forward model embedded in φ-IASI is called σ-IASI [3]. This is a monochromatic forward module using a look-up table for the optical depth. The look-up table is derived from LBLRTM (Line-by-Line Radiative Transfer Model) model [23]. For the work here shown we have used LBLRTM version 12.2. The forward module is based on 60 pressure layers, spanning the atmosphere from the ground level to the top assumed to be at 0.005 hPa. The model computes spectral radiances and analytical Jacobian derivatives of any surface and/or atmospheric parameter. IASI radiances are obtained through convolution with the IASI Instrumental Spectral Response Function (ISRF).

2.3. The EOF Module. The EOF module is a statistically based algorithm for the retrieval of the thermodynamic state of

the atmosphere (T_s, T, H_2O, and O_3). The general analytic formulation of the problem is described in the work of Serio et al. [24], which the interested reader is referred to for more details. Basically, the module is based on a linear regression among atmospheric parameters and radiances, represented through a truncated expansion of EOF scores. In fact, the radiances are first transformed to EOF scores and a truncated expansion is used to reduce the dimensionality of the data space. The regression coefficients are computed on the basis of a suitable training data set. For the current implementation we use a set of (T_s, T, H_2O, O_3) state vectors derived from the ECMWF (European Centre for Medium-Range Weather Forecasts) analysis for July 2010. A total of 1147 state vectors were used, which uniformly cover the Mediterranean basin.

2.4. The δ-IASI Module. The δ-IASI module [4] implements an iterative algorithm for the optimal estimation of the thermodynamic state of the atmosphere. The algorithms simultaneously retrieves the state vector $\mathbf{v}$ which, for sea surface, is made up of (T_s, T, H_2O, O_3). For sea surface emissivity we use the Masuda model [25].

The retrieval algorithm follows Rodgers optimal estimation [26] and uses an additional regularization parameter which improves the retrieval accuracy and convergence rate of the inverse scheme [15, 21]. The optimal estimator we use to get an estimate of the state vector $\mathbf{v}$ from spectral radiances has been first derived by Carissimo et al. [4] and discussed at length by Grieco et al. [21] and Masiello et al. [27].

The δ-IASI estimator reads

$$\left(\gamma \mathbf{S}_a^{-1} + \mathbf{K}^t \mathbf{S}_\varepsilon^{-1} \mathbf{K}\right) \mathbf{x} = \mathbf{K}^t \mathbf{S}_\varepsilon^{-1} \mathbf{y}, \tag{1}$$

where the superscript t indicates the transpose operation. Without any loss of generality, we assume that we are in a region around the first guess in which problem (1) is linear. If not, the scheme has to be further iterated according to the usual Gauss-Newton scheme [4]. With this in mind, in (1), we have

$$\begin{aligned} &\mathbf{x} = \hat{\mathbf{v}} - \mathbf{v}_a; \\ &\mathbf{y} = \left(\mathbf{R} - \mathbf{r}_0\right) - \mathbf{K}\mathbf{x}_a; \quad \text{with } \mathbf{x}_a = \mathbf{v}_a - \mathbf{v}_0, \end{aligned} \tag{2}$$

where $\hat{\mathbf{v}}$, $\mathbf{v}_a$, and $\mathbf{v}_0$ are the parameters' state vector (estimated), the *a priori* or background vector, and the first guess state vector (the size of these vectors will be denoted by N). Furthermore, $\mathbf{S}_\varepsilon$ in (1) is the observational covariance matrix and $\mathbf{S}_a$ indicates a suitable smoothing operator, normally fixed to the covariance matrix of $\mathbf{v}_a$ (e.g., [26]). $\mathbf{R}$ is the vector (size M) of observed radiances, $\mathbf{r}_0 = F(\mathbf{v}_0)$, with F being the forward model. Furthermore, the $M \times N$ derivative matrix or Jacobian derivative, $\mathbf{K}$, is computed as

$$\mathbf{K} = \left.\frac{\partial F(\mathbf{v})}{\partial \mathbf{v}}\right|_{\mathbf{v}=\mathbf{v}_0}. \tag{3}$$

If we define

$$\widetilde{\mathbf{S}}_\varepsilon = \gamma \mathbf{S}_\varepsilon, \tag{4}$$

then (e.g., [21]) (1) can be written in the equivalent form

$$\left(\mathbf{S}_a^{-1} + \mathbf{K}^t \widetilde{\mathbf{S}}_\varepsilon^{-1} \mathbf{K}\right) \mathbf{x} = \mathbf{K}^t \widetilde{\mathbf{S}}_\varepsilon^{-1} \mathbf{y}, \tag{5}$$

which says that scaling the background covariance by $1/\gamma$ has the same effect as scaling the observational covariance matrix by γ.

The meaning and use of the parameter γ have been discussed at length by Carissimo et al. [4] and Grieco et al. [21]. Basically, γ can improve the regularization of the inverse problem (1) and its tuning may allow us to trade off between accuracy and stability of the solution, $\hat{\mathbf{v}}$.

In fact, introducing the operator [4]

$$\mathbf{G} = \mathbf{S}_\varepsilon^{-1/2} \mathbf{K} \mathbf{S}_a^{1/2}, \tag{6}$$

the δ-IASI estimator can be put in the dimensionless form

$$\left(\mathbf{G}^t \mathbf{G} + \gamma \mathbf{I}\right) \mathbf{u} = \mathbf{G}^t \mathbf{z}; \quad \text{with } \mathbf{z} = \mathbf{S}_\varepsilon^{-1/2} \mathbf{y};\ \mathbf{u} = \mathbf{S}_a^{-1/2} \mathbf{x}, \tag{7}$$

whose solution, $\mathbf{u}$, is given by

$$\mathbf{u} = \mathbf{T}\mathbf{z} \tag{8}$$

with

$$\mathbf{T} = \left(\mathbf{G}^t \mathbf{G} + \gamma \mathbf{I}\right)^{-1} \mathbf{G}^t. \tag{9}$$

Equation (7) describes a Tikhonov-type or *ridge regression* regularization problem. According to Tikhonov and Arsenin (see, e.g., [28]) the operator $\mathbf{T}$ describes a regularization scheme with the norm of $\mathbf{T}$ given by

$$\text{norm}(\mathbf{T}) \leq \frac{1}{2\sqrt{\gamma}}. \tag{10}$$

Within the context of Tikhonov theory [28], the regularization of the problem (7) (hence (1)) improves for $\gamma > 1$. From (10) it is also seen that the amount of smoothing (regularization) is independent of the details of $\mathbf{S}_\varepsilon$ and $\mathbf{S}_a$, provided that they have inverse (so that we can define the operator $\mathbf{G}$). This is an important aspect of the inverse problem (1) because normally both $\mathbf{S}_\varepsilon$ and $\mathbf{S}_a$ are model approximations of the *truth*. Of course, the accuracy with which both $\mathbf{S}_\varepsilon$ and $\mathbf{S}_a$ are known affects the final estimate $\hat{\mathbf{v}}$ and its error analysis.

Finally, we stress that (7) also provides a fast and effective scheme for the computation of the estimate $\hat{\mathbf{v}}$. Based on the operator $\mathbf{G}$ and (7) an algorithm can be developed [4, 21], which does not require the inversion of $\mathbf{S}_a$ and, in case $\widetilde{\mathbf{S}}_\varepsilon$ is diagonal, is fast and accurate because it just requires the singular value decomposition of the kernel $\mathbf{G}^t\mathbf{G}$.

2.5. The Minor and Trace Gases Modules: The FTS-PSI Based Retrieval Technique. The PSI based retrieval technique consists in transforming the radiance spectrum into the interferogram domain where we identify a region which is particularly sensitive to the geophysical parameter we want to retrieve. Once the resonant peak in the interferogram domain has been identified, the given gas is simultaneously retrieved

with the most important interfering parameters, normally (T_s, T, H_2O).

The PSI technique has been applied in several contexts and is particularly efficient when information content related to the given geophysical parameter is confined to a small portion of the interferogram radiance. This is the case, for example, of linear molecules, such as CO and CO_2. In fact, the regularly spaced CO_2 absorption lines around 15 μm and of CO around 4.65 μm yield a resonant peak in the interferogram domain. To exemplify let us consider the case of CO. For CO the radiance spectrum shows a regular line spacing of ≈3.6 cm^{-1}; therefore, if we Fourier-transform the spectrum to the interferogram domain, we expect a resonant peak at an optical path difference (opd) of about the inverse of this value, that is, 0.28 cm. In order to better clarify this aspect, Figure 2 shows the interferogram around the expected resonance peak of CO for the US standard atmospheric profile [29] and for the same profile with a null concentration of CO. It can be seen that in the optical path difference interval between 0.2 and 0.3 the two interferograms are sensibly different, while they are quite similar outside this interval. This is an extreme example which gives an idea of the sensitivity of the interferogram radiance to the CO concentration near to the expected resonance peak.

The most important advantage of this technique is the improvement of the signal to noise ratio and the reduction of the influence of the interfering parameters in the final retrieval. The basics of the technique may be found in the work of Grieco et al. [20] and are here briefly summarized for the benefit of the reader.

For the purpose of the retrieval problem, the retrieved atmospheric parameters (these include the given gas and the set of the most important interfering factors, i.e., T_s, T, and H_2O) are represented through a parametric form of the profile:

$$q_i(p) = q_{0i}(p)\left(1 + f_{q_i}\right); \quad i = 1, \ldots, n, \tag{11}$$

where n is the number of parameters to be retrieved, q_i is the vertical profile, p is the atmospheric pressure, q_{0i} is a suitable first guess profile, and f_{q_i} is the parameter to be retrieved. For the case of surface temperature, (11) just reduces to the scalar form

$$T_s = T_{s0}\left(1 + f_{T_s}\right). \tag{12}$$

Considering the first-order Taylor expansion of the interferogram radiance $\mathbf{I}$ around first guess values, we have

$$\Delta\mathbf{I} = \mathbf{I} - \mathbf{I}_0 = \sum_{i=1}^{n} \mathbf{J}_i \mathbf{q}_{0i} f_{q_i}, \tag{13}$$

where, as for the radiance case, $\mathbf{I}$ is the observed interferogram, $\mathbf{I}_0$ is the interferogram computed with the forward model at the first geuss state vector, and $\mathbf{J}_i$ is the Jacobian derivative of the interferogram radiance.

Equation (13) can be rearranged as follows [20]:

$$\Delta\mathbf{I} = \mathbf{A}\mathbf{f}, \tag{14}$$

where $\mathbf{A}$ is the horizontal concatenation of $\mathbf{J}_i\mathbf{q}_{0i}$, $i = \ldots, n$.

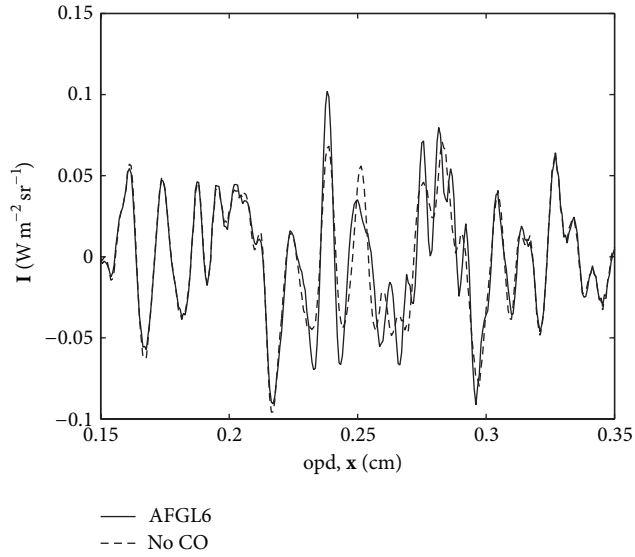

Figure 2: Interferogram radiance ($\mathbf{I}$) around the expected resonance peak of CO in Wm^{-2}sr^{-1}. The optical path difference (opd) is expressed in cm. AFGL6 stands for the US standard atmosphere, while "no CO" refers to the same atmospheric profile with a null CO concentration.

The vector $\mathbf{f}$ is retrieved by means of an unconstrained least square algorithm, and an estimation of the total columnar content is carried out according to

$$\widehat{Q}_i = \left(1 + \widehat{f_{q_i}}\right) \int_{p_s}^{0} q_i(p)\, dp, \tag{15}$$

where $\widehat{f_{q_i}}$ is the estimate of f_{q_i} and p_s is the surface pressure.

The usual least square *a posteriori* error analysis allows assessing the accuracy of the retrieval and the relative weight of the interfering parameters. Based on the *a posteriori* retrieval accuracy analysis, we have that the retrieved columnar content of the trace and minor gases has the error bars shown in Table 1. The details about the assessment of these values can be found in the work of Grieco et al. [20].

Figure 3 exemplifies the Jacobian derivative for CO mixing ratio, in the region around the interferogram resonant peak. The Jacobian derivative does not show any sharp peak all over the absorption spectral interval and most of the contribution comes from the pressure interval between 800 and 200 mb, which corresponds approximately to the region of the free troposphere. Similar results hold for the other gases considered in this study and are not shown for the sake of brevity.

3. Application to the Mediterranean Basin

The φ-IASI package has been applied to a dataset of ≈35000 IASI radiance spectra acquired over the Mediterranean basin for July 2010. This month has been selected because of the weather pattern over the Mediterranean region, which has been characterized by above normal surface temperatures associated with a relatively high frequency of blocking days.

Table 1: Accuracy of the retrieved total columns of the trace and minor gases for a single IASI field of view.

Gas species	Absolute accuracy	Relative accuracy
CO_2	±3 ppmv	<1%
CO	±1.5 ppbv	≈1.5%
CH_4	±13 ppbv	<1%
N_2O	±15 ppbv	≈5%

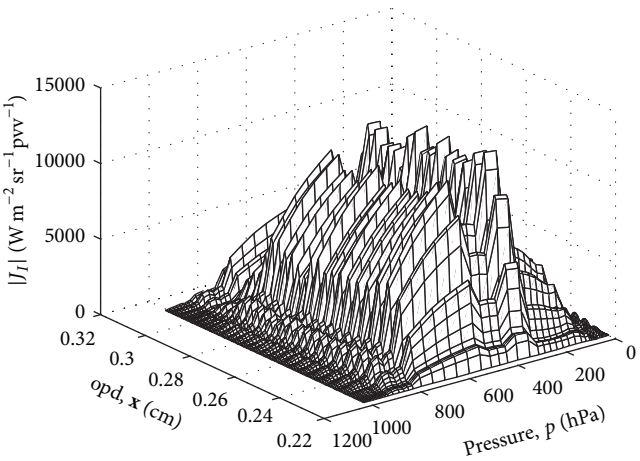

Figure 3: Mesh surface of J_I. The Jacobian derivative of the interferogram radiance with respect to the mixing ratio profile of CO.

Likewise, a particularly long blocking event has been experienced over Western Russia that has led to the occurrence of anomalously high temperatures over this region [30, 31]. Apart from the high temperatures, July 2010 showed the typical synoptic conditions [32, 33] of the Mediterranean summer (June to September), with high pressure over the Mediterranean Europe and a low-pressure through extending from the Persian Gulf through Iraq to the southeastern Mediterranean (see Figure 4).

It is now very well understood (e.g., Karnieli et al. [34] and the references therein) that this kind of weather pattern yields persistent northwesterly winds which causes long-range transport of air masses from southeastern and southwestern Europe into the eastern Mediterranean basin.

Arguing that atmospheric heavy molecules, such as CO_2 and NO_2, follow the dominant atmospheric circulation, Chahine et al. [7] demonstrated that satellite derived CO_2 data track weather patterns and can also be used to study the vertical and horizontal transports in the Earth atmosphere. Thus, according to Chahine et al. [7], because of the aforementioned summer weather pattern over the Mediterranean basin, we expect that CO_2 and N_2O should show a northwestern to southeastern pattern over the Mediterranean region. To study this effect, in this section, we will show and analyze trace gases retrievals form IASI data for July 2010.

To begin with, we briefly show and discuss patterns associated with retrievals of surface (T_s) and atmospheric parameters (T and O_3) derived with δ-IASI. Figures 5 and 6 show the maps of the retrieved atmospheric 500 hPa

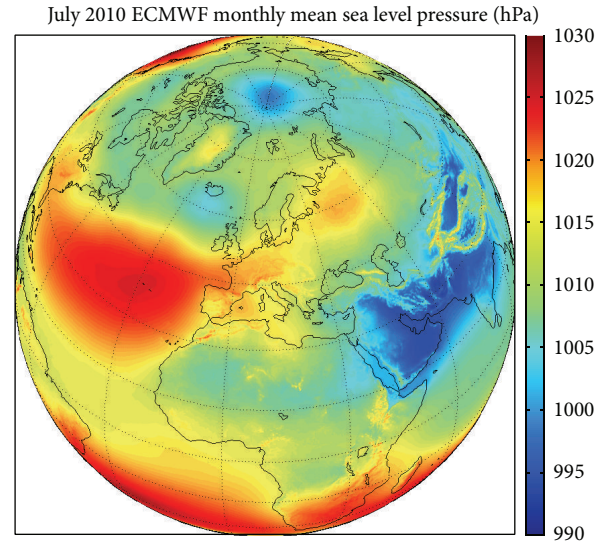

Figure 4: ECMWF analysis of the monthly sea level pressure for July 2010.

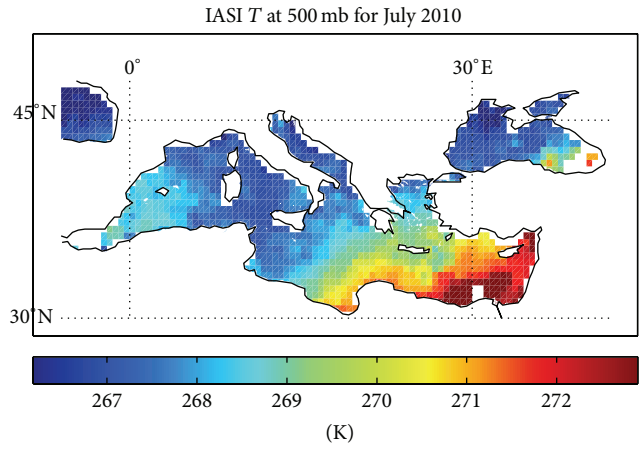

Figure 5: Retrieved atmospheric temperature at 500 mb for the month of July 2010. Data have been smoothed and rendered on a grid of 0.5° × 0.5° (lat. × lon.).

temperature and the total columnar ozone, averaged over the whole July period. These maps and all the following ones have been smoothed with a median filter and rendered on a regular grid of 0.5° × 0.5°. The value of each image pixel is the median value of the whole month distribution of all the values in the 2 × 2 neighborhood pixels around the corresponding pixel in the input image. The maps clearly show the transition from the European midlatitude air mass type to tropical one which characterizes the southeastern region of the Mediterranean basin. This transition is very well evidenced in the temperature and ozone maps and also testifies the quality of the retrieval. In addition, Figure 7 shows the sea surface temperature, with the expected northwestern southeastern gradient. This map evidences the relatively high sea surface temperature, which in most part of the Mediterranean basin exceeds 26°C (299 K).

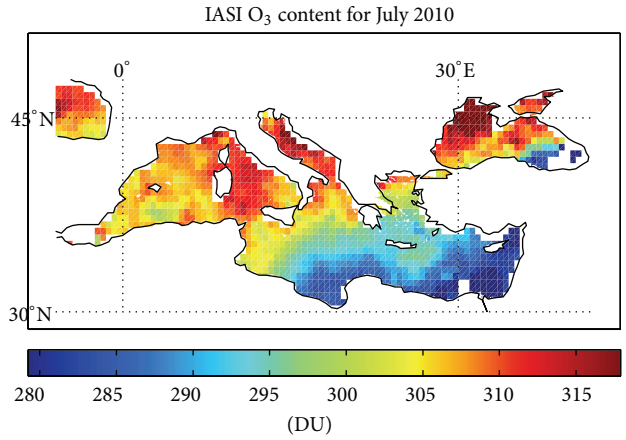

Figure 6: Retrieved atmospheric ozone content for the month of July 2010. Data have been smoothed and rendered on a grid of 0.5° × 0.5° (lat. × lon.).

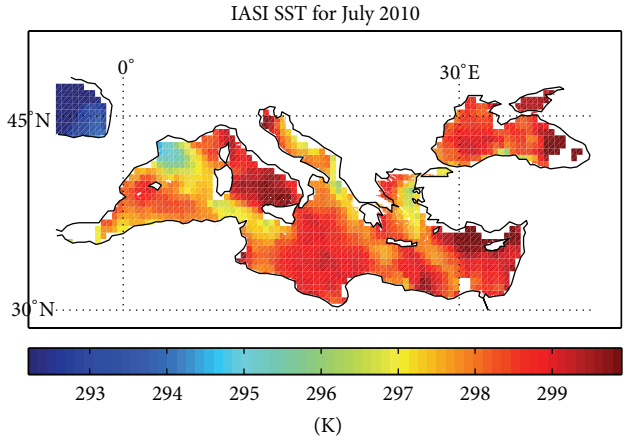

Figure 7: Retrieved sea surface temperature for the month of July 2010. Data have been smoothed and rendered on a grid of 0.5° × 0.5° (lat. × lon.).

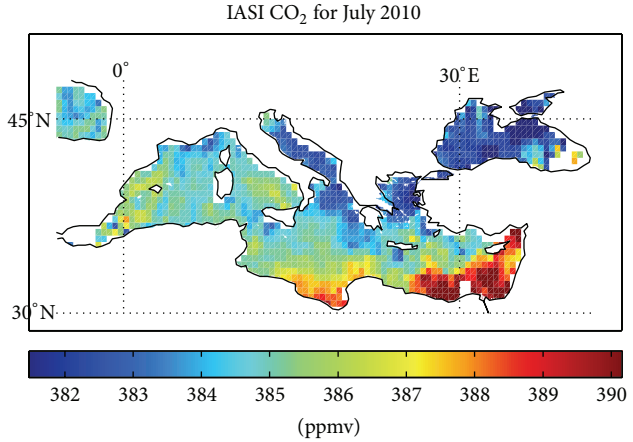

Figure 8: Retrieved tropospheric CO_2 content for the month of July 2010. Data have been smoothed and rendered on a grid of 0.5° × 0.5° (lat. × lon.).

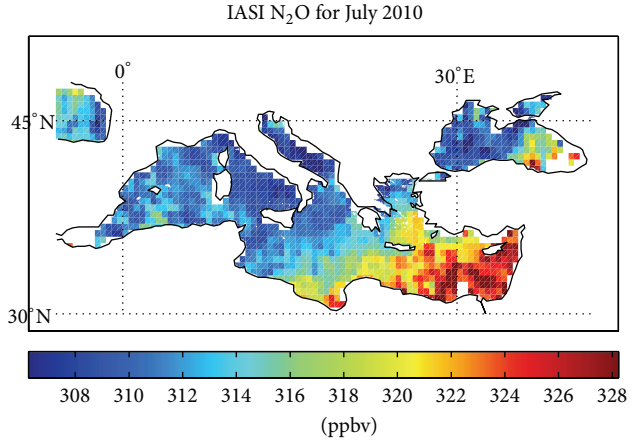

Figure 9: Retrieved tropospheric N_2O content for the month of July 2010. Data have been smoothed and rendered on a grid of 0.5° × 0.5° (lat. × lon.).

Figure 8 shows the retrieved tropospheric CO_2 content averaged over the whole period of July 2010. The most striking feature in this map is the marked northwestern-southeastern gradient, which is consistent with the large scale synoptic weather pattern for July 2010. Thus, Figure 8 supports Chahine et al.'s [7] finding that the retrieved CO_2 is capable of tracking the dominant atmospheric circulation. Similar results have been also found for N_2O (see Figure 9) and for methane (see Figure 10).

Finally, we show and discuss the comparison with in situ observations from the GAW stations of Begur (Spain), Lampedusa (Italy), Finokalia (Greece), Cairo (Egypt), and Sde Boker (Israel). It is important to remark that this comparison is not aimed at validating the retrievals. This matter has been addressed by Grieco et al. [20, 35], and the references therein. The present comparison is aimed at getting insight into understanding whether patterns and structures seen from satellite data are also shown by in situ observations.

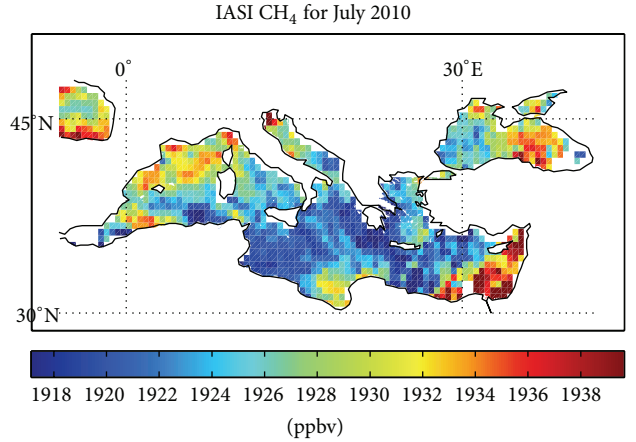

Figure 10: Retrieved tropospheric CH_4O content for the month of July 2010. Data have been smoothed and rendered on a grid of 0.5° × 0.5° (lat. × lon.).

Table 2: Time averaged values of the ground measurements (GM) and retrieved (IASI) columnar tropospheric content of trace gases.

	Begur		Lampedusa		Finokalia		Sde Boker		Cairo	
	GM	IASI	GM	IASI	GM	IASI	GM	IASI	GM	IASI
CO_2 (ppmv)	385.7	382.5	385.7	386.8	383.5	386.4	—	—	386.8	392.1
CH_4 (ppbv)	1834	1920	1860	1924	1865	1930	1890	1936	—	—

As already mentioned, these stations belong to the Global Atmosphere Watch (GAW) network and the data have been downloaded from the website of the World Data Centre for Greenhouse Gases. Figure 11 shows the geographical positions of the GAW stations. As it can be seen, they span all the Mediterranean basin. Three of them are seaside while Sde Boker and Cairo are about 100 Km far from the coast.

Table 2 compares the monthly average of in situ and IASI retrievals. The comparison is limited to CO_2 and CH_4 because these two gases have the largest density of monitoring (4 out of 5 GAW stations). There is a general consistency between in situ and satellite observations. However, systematic differences appear, which nevertheless are still consistent with the diverse atmospheric column sensed with in situ and satellite instruments. In fact, from Figure 3, we see that, conversely to in situ observations, IASI retrieval for atmospheric gases is sensitive to the free troposphere and cannot see the planetary boundary layer.

From the comparison of in situ observations and colocated satellite retrievals it can be seen that CO_2 and CH_4 concentrations tend to agree in showing a southeastward gradient, although it is fair to say that the gradient is much more marked for the satellite retrieval than in situ observations.

3.1. Performance of the Code. The performance of the code has been evaluated on a multiprocessor machine equipped with 6 physical and 6 virtual Intel i7 CPUs with a CPU clock rate equal to 3.33 GHz and a RAM memory which amounts to 24 GB. The time to invert a single IASI spectrum varies from about 8 seconds to 14 seconds, depending on the number of iterations the δ-IASI module performs. For the application discussed in this paper, the number of iterations ranges from 1 to 3 with an average number which is around 1.5. Obviously, the number of iterations depends on the quality of the first guess of the thermodynamic state of the atmosphere and this aspect is crucial for both the quality and the speed of the retrieval. For the application under examination, we can consider that the average time spent for the retrieval of a single IASI spectrum is about 10 seconds. Considering that the total number of IASI spectra over the Mediterranean basin for the whole month of July is about 35000 and that only about the 25% of the spectra have been classified as clear-sky and therefore processed by the physical inversion scheme, the computational time spent for the retrieval amounts to a little bit more than 24 hours. The availability of 6 physical CPUs reduced this time to few hours. Considering the implementation of the code for the whole globe, a number of 50 to 100 CPUs of the type described above should be enough to guarantee operability.

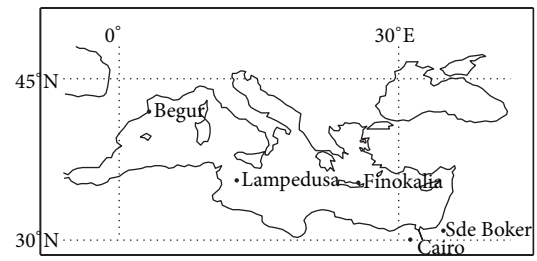

Figure 11: Map of the GAW stations.

The hardware equipment used for the evaluation of the performance of the code is available at the moment for few thousand Euros, which means that the computer technology is now mature enough and contextually cheap to allow the full exploitation of information content of hyperspectral satellite infrared sounders such as a IASI.

4. Conclusions

The operational implementation of the φ-IASI software package over the Mediterranean basin for the retrieval of the thermodynamic state of the atmosphere and of the free tropospheric columnar content of CO_2, CO, CH_4, and N_2O from the hyperspectral radiance measurements acquired by the Infrared Atmospheric Sounding Interferometer has been presented.

We have shown that φ-IASI can operationally retrieve skin temperature, T_s atmospheric parameters (T, H_2O, and O_3), and minor and trace gases, namely, CO, CO_2, N_2O, and CH_4, at the scale of the Mediterranean basin.

The retrieval scheme has been exemplified through its application to IASI spectra recorded on July 2010. The retrieval results have been also compared to in situ observations from five GAW permanent stations. Considering that nadir-looking IASI retrievals are sensitive to the free troposphere, whereas in situ measurements sense the boundary layer, the comparison has shown a fair agreement of in situ observations with IASI observations. IASI retrieval for heavy molecules, noticeably CO_2 and N_2O, shows marked northwestern to southeastern gradients with a relatively higher concentration over the eastern part of the Mediterranean basin. This behaviour is both consistent with biogenic activity of the Mediterranean sea [36] and the large scale synoptic weather circulation in July 2010 which transports air masses from southeastern and southwestern Europe into the eastern Mediterranean basin.

Our findings support previous results for CO_2 geospatial distribution [7] and also exemplify how satellite retrievals are complementary to in situ observations to study the vertical and horizontal transports in the Earth's atmosphere of gases such as CO_2, N_2O, and CH_4 which are of paramount interest in view of their crucial role within the anthropogenic greenhouse effect and hence global warming of the planet.

Conflict of Interests

The authors declare that there is no conflict of interests regarding the publication of this paper.

Acknowledgments

The measurements in Lampedusa and Sde Boker have been downloaded from the web page http://www.esrl.noaa.gov/gmd/dv/iadv/ owned by NOAA/ESRL. The measurements in Begur and Finokalia have been supplied by the Laboratoire des Sciences du Climat et de l'Environnement (http://www.lsce.ipsl.fr/). The measurements in Cairo have been supplied by the Egyptian Meteorological Authority (http://ema.gov.eg/). This work has been partly supported by *The RITMARE Flagship Project* (CNR-MIUR). IASI has been developed and built under the responsibility of the Centre National d'Etudes Spatiales (CNES, France). It is flown onboard the Metop satellites as part of the EUMETSAT Polar System. The IASI L1 data are received through the EUMETCast near real time data distribution service.

References

[1] F. Hilton, R. Armante, T. August et al., "Hyperspectral earth observation from IASI: five years of accomplishments," *Bulletin of the American Meteorological Society*, vol. 93, no. 3, pp. 347–370, 2012.

[2] G. Masiello, C. Serio, A. Carissimo, G. Grieco, and M. Matricardi, "Application of φ-IASI to IASI: retrieval products evaluation and radiative transfer consistency," *Atmospheric Chemistry and Physics*, vol. 9, no. 22, pp. 8771–8783, 2009.

[3] U. Amato, G. Masiello, C. Serio, and M. Viggiano, "The σ-IASI code for the calculation of infrared atmospheric radiance and its derivatives," *Environmental Modelling & Software*, vol. 17, no. 7, pp. 651–667, 2002.

[4] A. Carissimo, I. De Feis, and C. Serio, "The physical retrieval methodology for IASI: The δ-IASI code," *Environmental Modelling and Software*, vol. 20, no. 9, pp. 1111–1126, 2005.

[5] H. Shimoda and T. Ogawa, "Interferometric monitor for greenhouse gases (IMG)," *Advances in Space Research*, vol. 25, no. 5, pp. 937–946, 2000, Remote Sensing and Applications: Earth, Atmosphere and Oceans.

[6] M. Chahine, C. Barnet, E. T. Olsen, L. Chen, and E. Maddy, "On the determination of atmospheric minor gases by the method of vanishing partial derivatives with application to CO_2," *Geophysical Research Letters*, vol. 32, no. 22, Article ID L22803, pp. 1–5, 2005.

[7] M. T. Chahine, L. Chen, P. Dimotakis et al., "Satellite remote sounding of mid-tropospheric CO_2," *Geophysical Research Letters*, vol. 35, no. 17, Article ID L17807, 2008.

[8] W. W. McMillan, C. Barnet, L. Strow et al., "Daily global maps of carbon monoxide from nasa's atmospheric infrared sounder," *Geophysical Research Letters*, vol. 32, no. 11, pp. 1–4, 2005.

[9] C. Crevoisier, A. Chédin, H. Matsueda, T. MacHida, R. Armante, and N. A. Scott, "First year of upper tropospheric integrated content of CO_2 from IASI hyperspectral infrared observations," *Atmospheric Chemistry and Physics*, vol. 9, no. 14, pp. 4797–4810, 2009.

[10] P. Ricaud, J.-L. Attié, H. Teyssèdre et al., "Equatorial total column of nitrous oxide as measured by IASI on MetOp-A: Implications for transport processes," *Atmospheric Chemistry and Physics*, vol. 9, no. 12, pp. 3947–3956, 2009.

[11] A. Boynard, C. Clerbaux, P.-F. Coheur et al., "Measurements of total and tropospheric ozone from IASI: comparison with correlative satellite, ground-based and ozonesonde observations," *Atmospheric Chemistry and Physics*, vol. 9, no. 16, pp. 6255–6271, 2009.

[12] L. Clarisse, P. F. Coheur, A. J. Prata et al., "Tracking and quantifying volcanic SO_2 with IASI, the September 2007 eruption at Jebel at Tair," *Atmospheric Chemistry and Physics*, vol. 8, no. 24, pp. 7723–7734, 2008.

[13] L. Clarisse, C. Clerbaux, F. Dentener, D. Hurtmans, and P.-F. Coheur, "Global ammonia distribution derived from infrared satellite observations," *Nature Geoscience*, vol. 2, no. 7, pp. 479–483, 2009.

[14] C. Clerbaux, A. Boynard, L. Clarisse et al., "Monitoring of atmospheric composition using the thermal infrared IASI/MetOp sounder," *Atmospheric Chemistry and Physics*, vol. 9, no. 16, pp. 6041–6054, 2009.

[15] G. Masiello and C. Serio, "Simultaneous physical retrieval of surface emissivity spectrum and atmospheric parameters from infrared atmospheric sounder interferometer spectral radiances," *Applied Optics*, vol. 52, no. 11, pp. 2428–2446, 2013.

[16] D. Hurtmans, P.-F. Coheur, C. Wespes et al., "FORLI radiative transfer and retrieval code for IASI," *Journal of Quantitative Spectroscopy and Radiative Transfer*, vol. 113, no. 11, pp. 1391–1408, 2012.

[17] T. Kerzenmacher, B. Dils, N. Kumps et al., "Validation of IASI FORLI carbon monoxide retrievals using FTIR data from NDACC," *Atmospheric Measurement Techniques*, vol. 5, no. 11, pp. 2751–2761, 2012.

[18] D. Wunch, P. O. Wennberg, G. C. Toon et al., "A method for evaluating bias in global measurements of CO_2 total columns from space," *Atmospheric Chemistry and Physics*, vol. 11, no. 23, pp. 12317–12337, 2011.

[19] T. G. Kyle, "Temperature soundings with partially scanned interferograms," *Applied Optics*, vol. 16, no. 2, pp. 326–333, 1977.

[20] G. Grieco, G. Masiello, M. Matricardi, and C. Serio, "Partially scanned interferogram methodology applied to IASI for the retrieval of CO, CO_2, CH_4 and N_2O," *Optics Express*, vol. 21, no. 21, pp. 24753–24769, 2013.

[21] G. Grieco, G. Masiello, M. Matricardi, C. Serio, D. Summa, and V. Cuomo, "Demonstration and validation of the φ-IASI inversion scheme with NAST-I data," *Quarterly Journal of the Royal Meteorological Society*, vol. 133, no. 3, pp. 217–232, 2007.

[22] U. Amato, L. Lavanant, G. Liuzzi et al., "Cloud mask via cumulative discriminant analysis applied to satellite infrared observations: scientific basis and initial evaluation," *Atmospheric Measurement Techniques*, vol. 7, no. 10, pp. 3355–3372, 2014.

[23] S. A. Clough, M. W. Shephard, E. J. Mlawer et al., "Atmospheric radiative transfer modeling: a summary of the AER codes,"

Journal of Quantitative Spectroscopy and Radiative Transfer, vol. 91, no. 2, pp. 233–244, 2005.

[24] C. Serio, G. Masiello, and G. Grieco, *EOF Expression Analytical Model with Applications to the Retrieval of Atmospheric Temperature and Gas Constituents Concentrations from High Spectral Resolution Infrared Observations*, chapter 2, Nova Science Publishers, 2013.

[25] K. Masuda, T. Takashima, and Y. Takayama, "Emissivity of pure and sea waters for the model sea surface in the infrared window regions," *Remote Sensing of Environment*, vol. 24, no. 2, pp. 313–329, 1988.

[26] C. D. Rodgers, *Inverse Methods for Atmopsheric Sounding: Theory and Practice*, vol. 2, World Scientific Publishing, Singapore, 2000.

[27] G. Masiello, C. Serio, and P. Antonelli, "Inversion for atmospheric thermodynamical parameters of IASI data in the principal components space," *Quarterly Journal of the Royal Meteorological Society*, vol. 138, no. 662, pp. 103–117, 2012.

[28] A. N. Tikhonov and V. Y. Arsenin, *Solutions of Ill-Posed Problems*, Winston& Sons, Washington, DC, USA, 1978.

[29] G. P. Anderson, S. A. Clough, F. X. Kneizys, J. H. Chetwynd, and E. P. Shettle, "Afgl atmospheric constituent profiles (0–120 km)," Tech. Rep., Air Force Geophysics Laboratory, Hanscom AFB, Bedford, Mass, USA, 1986.

[30] D. Barriopedro, E. M. Fischer, J. Luterbacher, R. M. Trigo, and R. García-Herrera, "The hot summer of 2010: redrawing the temperature record map of Europe," *Science*, vol. 332, no. 6026, pp. 220–224, 2011.

[31] B. A. Revich, "Heat-wave, air quality and mortality in european russia in summer 2010: preliminary assessment," *Human Ecology*, no. 7, pp. 3–9, 2011.

[32] Great Britain Meteorological Office, *Weather in the Mediterranean*, Great Britain Meteorological Office, London, UK, 2nd edition, 1962.

[33] Y. Goldreich, *The Climate of Israel: Observation, Research and Applications*, Springer, New York, NY, USA, 2003.

[34] A. Karnieli, Y. Derimian, R. Indoitu et al., "Temporal trend in anthropogenic sulfur aerosol transport from central and eastern Europe to Israel," *Journal of Geophysical Research D: Atmospheres*, vol. 114, no. 15, Article ID D00D19, 2009.

[35] G. Grieco, G. Masiello, C. Serio, R. L. Jones, and M. I. Mead, "Infrared atmospheric sounding interferometer correlation interferometry for the retrieval of atmospheric gases: the case of H_2O and CO_2," *Applied Optics*, vol. 50, no. 22, pp. 4516–4528, 2011.

[36] F. D'Ortenzio, D. Antoine, and S. Marullo, "Satellite-driven modeling of the upper ocean mixed layer and air-sea CO_2 flux in the Mediterranean Sea," *Deep Sea Research Part I: Oceanographic Research Papers*, vol. 55, no. 4, pp. 405–434, 2008.